BIOSCIENCE JOURNAL

REMOTE SENSING IN THE ESTIMATION OF EVAPOTRANSPIRATION OF TOMATO CULTIVATION FOR INDUSTRIAL PROCESSING

Carolina Carvalho Rocha SENA[1], José ALVES JÚNIOR[1], João Maurício Fernandes SOUZA[2], Adão Wagner Pêgo EVANGELISTA[1], Rafael BATTISTI[1], Derblai CASAROLI[1], Elson de Jesus ANTUNES JUNIOR[2]

[1]College of Agronomy, Universidade Federal de Goiás, Campus Samambaia, Goiânia, Goiás, Brazil.
[2]Anapolis University Center, UniEvangélica, Agronomy, Anápolis, Goiás, Brazil.

Corresponding author:
Carolina Carvalho Rocha Sena
eng.carolinasena@gmail.com

How to cite: SENA, C.C.R., et al. Remote sensing in the estimation of evapotranspiration of tomato cultivation for industrial processing. *Bioscience Journal*. 2025, **41**, e41002. https://doi.org/10.14393/BJ-v41n0a2025-70757

Abstract

This study evaluated the performance of the SAFER and METRIC algorithms to estimate the actual evapotranspiration (ET_a) of irrigated tomato crops for industrial processing in the south-central region of Goiás, Brazil. The research was conducted in eight tomato-producing areas using center-pivot irrigation during the 2018 and 2019 harvests. Landsat 8 OLI/TIRS satellite images (temporal resolution of 16 days) helped estimate ET_a through the SAFER e METRIC models compared with FAO methods, using the single crop coefficient (K_c) of the FAO-56/Embrapa and the soil water balance (BHS) method based on statistical indices. The analyzed algorithms presented spatiotemporal variations for ET_a during the tomato crop cycle for industrial processing. The maximum evapotranspiration estimated by SAFER was 5.20 mm d^{-1}, and by METRIC was 5.00 mm d^{-1}. The algorithms were accurate compared with the standard methods, mainly the FAO using Embrapa's K_c. The mean squared error was lower than 0.59 mm d^{-1} for SAFER and lower than 0.73 mm d^{-1} for METRIC. The ET_a estimated by both models in the vegetative and fructification phases was lower than the mean absolute error of 0.24 mm d^{-1} compared with the standard methods. The SAFER model showed higher agreement with standard practices than the METRIC model, with an index between 0.64 and 0.99. This study demonstrated that algorithms may effectively estimate ET_a in tomato crops for industrial processing in the analyzed region.

Keywords: Center pivot. Geoprocessing. *Solanum lycopersicum* L. Water management.

1. Introduction

Using water resources for agriculture tends to increase with population growth due to the characteristics of the new agricultural frontiers and the decreased reliability of natural supplies (Pires et al. 2016; Petropoulos et al. 2018). This growing water usage prompts the need for integrated and participative solutions to manage drainage basins and mainly efficient and rational water use for irrigation (Saccon 2018; Singh 2018).

Hence, reliable estimates of the hydrological cycle's components, such as crop water requirements, are essential for efficient irrigation systems and hydrological models (Allen et al. 1998; Pires et al. 2016). Estimating crop water requirements through meteorological monitoring by evapotranspiration (ET) and single crop coefficient (K_c) is among the most traditional and frequent irrigation management practices.

However, the logistic challenges and high installation costs of some standard methods to determine ET and spatiotemporal variability from the dependence on these soil and vegetation characteristics allow ET estimation only in small areas. That makes climate monitoring an obstacle for irrigation management (Allen et al. 1998; Wagle et al. 2019).

Thus, remote sensing to estimate ET becomes promising for irrigation management. It estimates the actual evapotranspiration (ET_a) of crops on a large spatiotemporal scale according to the origin of images, regardless of the crop, phenological phase, and crop system. Remote sensing is also an alternative for regions with difficult access and missing data due to high machinery costs (Singh 2016; Zhang et al. 2016; Dias et al. 2021).

Some models have excelled in estimating ET_a by satellite images in agriculture (Venancio et al. 2020; Xue et al. 2020). Among them are the Two-Source Energy Balance (TSEB) (Norman and Becker 1995), Surface Energy Balance Algorithm for Land (SEBAL) (Bastiaanssen et al. 1998), Mapping Evapotranspiration at high Resolution with Internalized Calibration (METRIC) (Allen et al. 2007), Simple Algorithm For Evapotranspiration Retrieving (SAFER) (Teixeira 2010; Teixeira 2012), and Operational Simplified Surface Energy Balance (SSEBop) (Senay et al. 2016). However, algorithm selection and whether remote sensing perceives alterations among crops, regions, and water availability remain to be studied.

The METRIC model uses reference evapotranspiration (ET_o) from meteorological data to calibrate sensible heat flux and extrapolate instantaneous values into daily values. This cold pixel calibration absorbs errors from the radiation balance and soil heat flux, eliminating the need for advanced atmospheric corrections of soil temperature and albedo (Allen et al. 2007). Nevertheless, this model is limited by the need to identify pixels in extreme water conditions in the image to calculate the sensible heat flux. When this calculation is made incorrectly, it may cause evapotranspiration estimation errors (Khand et al. 2017; Elkatoury et al. 2019).

The SAFER model is based on ET_a and ET_o ratio modeling, measured by the Penman-Monteith equation (Teixeira 2012; Teixeira et al. 2013). This model does not require identifying anchor pixels. It estimates ET with agrometeorological data from stations, whether automatic or conventional (Teixeira et al. 2013), even though it needs calibrating coefficients *a* and *b* to measure ET/ET_o (Venancio et al. 2021).

Tomatoes (*Solanum lycopersicum* L.) are the most widespread vegetable produced worldwide after potato crops. They are relevant to human health because they are a source of lycopene, which prevents diseases and heart conditions (Breksa et al. 2015).

Brazil is the eighth largest tomato producer for industrial processing (1.45 million tons), ranking behind countries such as the United States, China, Italy, and Spain, with 11.43, 5.18, 4.84, and 2.95 million tons, respectively (WPTC 2020). Goiás is Brazil's largest producer of tomatoes for industrial processing, showing relevance to Brazilian agribusiness (IBGE 2019).

The tomato plant is one of the most demanding in terms of water, with a mean consumption between 300 and 650 mm. Its cultivation in Goiás is entirely irrigated (Feb-Oct), mainly using a center pivot, making irrigation management essential for crop success (Marouelli et al. 2012). However, it is usually performed inadequately (Marouelli and Silva 2006; Basílio et al. 2019). Thus, empirical irrigation management studies are needed to verify the efficiency and modernization of the productive system.

Therefore, this study evaluated the SAFER and METRIC algorithm performances in estimating the ET_a of tomatoes for industrial processing with center-pivot irrigation in the south-central region of Goiás, Brazil.

2. Material and Methods

Study area and crop data

The study was conducted in five areas (Figure 1), with three having two repeated crops of tomato production for industrial processing with center-pivot irrigation in Goiás. The locations were Palmeiras de Goiás (16°41'45" S, 49°53'05" W, 670 m), Anápolis (16°26'18" S, 48°50'18" W, 1002 m), Silvânia (16°45'57" S, 48º40'05" W, 960 m), Gameleira de Goiás (16º22'43" S, 48º37'11" W, 975 m), and Piracanjuba (17°32'24" S, 48°56'29" W, 690 m). The study occurred during the 2018 and 2019 harvests. The Köppen-

Geiger classification defines the region's climate as Aw – tropical, with dry winters and rainy summers, average annual precipitation of 1500 mm, and an average annual temperature of 23.4°C (Kottek et al. 2006; Cardoso et al. 2014).

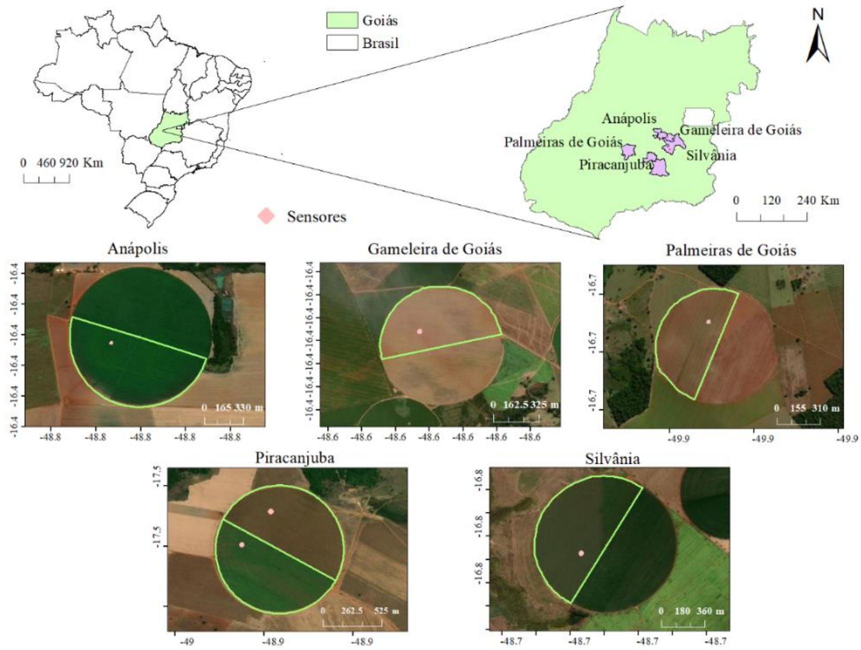

Figure 1. Localization of the studied areas, emphasizing the installation site of soil moisture sensors and rain gauges: Palmeiras de Goiás (16°41'45" S, 49°53'05" W, 670 m), Anápolis (16°26'18" S, 48°50'18" W, 1002 m), Silvânia (16°45'57" S, 48º40'05" W, 960 m), Gameleira de Goiás (16º22'43" S, 48º37'11" W, 975 m), and Piracanjuba (17°32'24" S, 48°56'29" W, 690 m).

The predominant soil of the studied regions was dystrophic Red Latosol (Oxisol) (EMBRAPA 2013). Table 1 describes the technical descriptions of the tomato crops for industrial processing in the analyzed areas.

Table 1. Technical description of the tomato crops for industrial processing in the analyzed areas.

Location	Area (ha)	Hybrid	Transplanting	Harvest	System*
Anápolis	50	N-901	05/15/2018	09/18/2018	NT
Palmeiras de Goiás	25	N-901	06/05/2018	09/22/2018	NT
Palmeiras de Goiás	25	N-901	06/17/2019	10/07/2019	NT
Piracanjuba	50	N-901	05/23/2019	09/24/2019	CT
Piracanjuba	50	CRV-2909	03/26/2019	07/15/2019	CT
Silvânia	50	N-901	08/05/2018	09/13/2018	CT
Silvânia	50	H-9553	05/26/2019	09/12/2019	NT
Gameleira de Goiás	25	CRV-6116	05/23/2018	09/13/2018	NT

*CT: Conventional tillage, NT: No-tillage.

Landsat 8 images

The study used images from the OLI/TIRS orbital sensors onboard the Landsat 8 satellite, with a multispectral spatial resolution of 30 m, thermal resolution of 100 m, and temporal resolution of 16 days of the orbit/point 221/72 and 222/72, Landsat Collection 1 Level 1. It also applied images of the digital elevation model (DEM) obtained by the Shuttle Radar Topography Mission (SRTM) of the areas of interest. Both image sets were collected from the image gallery of the United States Geological Survey (USGS, 2020). The area located in Anápolis presented an image overlay, which reduced the temporal resolution to 8 days. Images with clouds were discarded.

Description of the METRIC model

The METRIC model used the methodology described by Allen et al. (2005), Allen et al. (2007), and Allen et al. (2011). The ET_a is estimated as the surface energy balance residue using Eq. 1:

$$LE = R_n - G - H \quad (1)$$

where LE is the latent heat flux - energy wasted in the evapotranspiration process (W m^{-2}), R_n is the net radiation (W m^{-2}), G is the soil heat flux (W m^{-2}), and H is the sensible heat flux in the air (W m^{-2}).

Eq. 2 measures net radiation (R_n):

$$R_n = RS\downarrow - \alpha RS\downarrow + RL\downarrow - RL\uparrow - (1-\varepsilon_0)\, RL\downarrow \quad (2)$$

where R_n is the net radiation (W m^{-2}), $RS\downarrow$ is the shortwave radiation input (W m^{-2}), α is the surface albedo (dimensionless), $RL\downarrow$ is the longwave radiation input (W m^{-2}), $RL\uparrow$ is the longwave radiation output (W m^{-2}), and εo is thermal surface emissivity (dimensionless).

Eq. 3 estimated soil heat flux (G):

$$\frac{G}{R_n} = T_s\,(0.0038 + 0.0074\,\alpha).(1 - 0.98 NDVI^4) \quad (3)$$

where G is the soil heat flux (W m^{-2}), T_s is the surface temperature (°C), α is the surface albedo, NDVI is the normalized difference vegetation index, and R_n is the net radiation (W m^{-2}).

Sensible heat flux (H) was measured with the following aerodynamic heat transfer using equation Eq. 4:

$$H = \rho_{air}\, C_p\, \frac{dT}{r_{ah}} \quad (4)$$

where ρ_{air} is air density (kg m^{-3}), C_p is specific air heat (1004 J K^{-1} kg^{-1}), dT is the temperature difference between two heights - z_1 (0.1 m) and z_2 (2 m), and r_{ah} is the aerodynamic resistance for heat transfer (s m^{-1}).

In the METRIC model, the Calibration using Inverse Modeling at Extreme Conditions (CIMEC) applied to the energy balance internally adjusts r_{ah} and dT values (Bastiaanssen et al. 1998; Allen et al. 2007). This calibration is based on the linear relationship between dT and T_s in two extreme conditions, i.e., between two anchor points. The cold anchor pixel is mainly represented by well-irrigated areas and soil entirely covered by vegetation. The maximum evapotranspiration is supposedly equivalent to the reference evapotranspiration multiplied by a constant coefficient. The hot pixel is mainly represented by areas in dry conditions, with little or no vegetation (exposed soil) and evapotranspiration close to zero (Allen et al. 2005; Allen et al. 2007).

Considering the latent heat flux, each pixel is calculated when the satellite passes over the area, and they are converted into instantaneous evapotranspiration (Eq. 5):

$$ET_{inst.} = 3600\, \frac{LE}{\lambda\, \rho_w} \quad (5)$$

where ET_{inst} is instantaneous ET (mm h^{-1}), LE is the latent heat flux consumed by ET (W m^{-2}), ρ_w is water density (1000 kg m^{-3}), 3600 is the conversion time from seconds to hours, and λ is the latent heat of vaporization (J kg^{-1}) measured by Eq. 6:

$$\lambda = (2.501 - 0.00236(T_S - 273.15) \times 10^6 \quad (6)$$

Fractional reference evapotranspiration (ET_rF) is measured using the data of the meteorological station close to the studied area (Eq. 7):

$$ET_rF = \frac{ET_{inst}}{ET_o} \quad (7)$$

where ET_{inst} is instantaneous evapotranspiration (mm h^{-1}), and ET_o is the reference evapotranspiration when the satellite passes over the area (mm h^{-1}).

Eq. 8 measured actual evapotranspiration obtained by METRIC (ET_a - ET_{METRIC}) :

$$ET_{METRIC} = ET_rF.\, ET_o \quad (8)$$

where ET_rF is fractional reference evapotranspiration, and ET_o is reference evapotranspiration - FAO 56 (mm d^{-1}).

Description of the SAFER model

The SAFER model used the methodology described by Teixeira (2010), Teixeira et al. (2012), and Teixeira et al. (2017). Eq. 9 calculated surface albedo values:

$$\alpha_o = 0.7 * \alpha_{top} + 0.06 \quad (9)$$

where α_o is the surface albedo, and α_{top} is the upper atmosphere albedo.

Eq. 10 measured the surface temperature:

$$T_o = 1.11 \times T_{bright} - 31.89 \quad (10)$$

where T_{bright} is determined by Eq. 11:

$$T_{bright} = \frac{\frac{1321.08}{\ln\left(\frac{774.89}{L_{10}+1}\right)} + \frac{1201.14}{\ln\left(\frac{480.89}{L_{11}+1}\right)}}{2} \quad (11)$$

where L is the radiance of thermal bands 10 and 11.

Eq. 12 measured the normalized difference vegetation index (NDVI):

$$NDVI = \frac{(IVP - V)}{IVP + V} \quad (12)$$

where IVP is the near-infrared band reflectance, and V is the red band reflectance.

Eq. 13 calculated the instantaneous values of the ET/ET_o relationship:

$$\frac{ET}{ET_o} = \exp\left[a + b\left(\frac{T_o}{\alpha_o \times NDVI}\right)\right] \quad (13)$$

where α_o is the surface albedo, T_o is the surface temperature (°C), ET_o is reference evapotranspiration (mm d^{-1}) by the Penman-Monteith method - FAO-56, and "a" and "b" are coefficients with values equal to 1.0 (Teixeira et al. 2013; Hernandez et al. 2016) and -0.008 (Teixeira, 2010), respectively.

Eq. 14 determined actual evapotranspiration by the SAFER model (ET_a – ET_{SAFER}):

$$ET_{SAFER} = \frac{ET}{ET_o} . ET_o \quad (14)$$

where ET_o is reference evapotranspiration - FAO 56 (mm d^{-1}).

Pixels were selected using the ET_a value (SAFER and METRIC) within the center-pivot area so that all images analyzed during the tomato crop cycle had equivalent locations. The control pixels were located in a 120m radius from the moisture sensor batteries installed in the studied area.

Soil water balance

Soil water storage measurement used the Simpson rule (Libardi, 2012), following Eq. 15:

$$ARM = \int_0^L \theta\,(Z)dZ = \frac{Z}{3}\ (\theta_0 + 4\theta_1 + \theta_2) \quad (15)$$

where ARM is soil water storage, Z is the effective depth of the root system, and θ is soil water content (m^3 m^{-3}) obtained through FDR soil moisture sensors (EC-5 of Decagon Devices), calibrated following Sena et al. (2020), in depths of 0.1 (θ_0), 0.3 (θ_1), and 0.5(θ_2) m, and connected to a Decagon Devices datalogger EM-50.

The ΔARM was determined by the difference in soil water content values obtained at the initial and final times of each period and expressed by Eq. 16:

$$\Delta ARM = \lfloor \theta_f - \theta_i \rfloor L = A_f - A_i \quad (16)$$

where A_f and A_i are the final and initial accumulated water storages, respectively.

Three FDR sensor batteries were installed in each analyzed area. The selected points for analyzing the current evapotranspiration estimate were close to sensor locations.

Reference evapotranspiration and single crop coefficient

The Penman-Monteith FAO standard method (Allen et al. 1998) determined ET_o, and the necessary meteorological data was obtained through automatic meteorological stations installed at a 50m radius in each studied area. The single crop coefficient (ET_{FAO}) (Allen et al. 1998) was determined using the coefficients recommended by Embrapa, the Brazilian Agricultural Research Corporation ($ET_{Embrapa}$) (Marouelli et al. 2012), according to the crop system (conventional or no-till) used in the studied area, as in Table 2.

Table 2. Tomato single crop coefficient (K_c) according to FAO and Embrapa.

Development stage	$K_{c\ FAO}$	$K_{c\ Embrapa\ CT}$	$K_{c\ Embrapa\ NT}$
Initial	0.6	0.80 - 0.90	0.35 - 0.45
Vegetative	1.15	0.55 - 0.65	0.40 - 0.50
Fructification	0.70 - 0.90	1.00 - 1.11	0.95 - 1.05
Maturation	0.6	0.25 - 0.35	0.25 - 0.35

CT: Conventional tillage, NT: No-tillage.

Statistics

The models were evaluated through linear regression analysis. They were statistical indicators, coefficient of determination (R^2) (Eq. 17), Willmott index of agreement (d) (Willmott et al. 1985) (Eq. 18), mean absolute error (MAE) (Eq. 19), and mean squared error (MSE) (Eq. 20).

$$R^2=1-\left[\frac{\sum (E_i - O_i)^2}{\sum (|E_i-O|+|O_i-O|)^2}\right] \quad (17)$$

$$d = 1-\left[\frac{\sum (E_i-O_i)^2}{\sum (|E_i-O|+|O_i-O|)^2}\right] \quad (18)$$

$$MAE=\frac{1}{N}\sum |O_i-E_i| \quad (19)$$

$$MSE = \frac{1}{n}\sum (O_i - E_i)^2 \quad (20)$$

where O_i is the observed value (ET determined by the FAO, Embrapa, and the BHS method) in mm d^{-1}, E_i is the value estimated by the SAFER and METRIC algorithms in mm d^{-1}, O is the mean of observed values in mm d^{-1}, and n is the number of observations.

3. Results

Figures 2, 3 and 4 present the spatiotemporal distribution of ET_a for the tomato crops measured by the SAFER (ET_{SAFER}) and METRIC (ET_{METRIC}) algorithms in the studied areas in 2018 and 2019.

ET_{SAFER} and ET_{METRIC} values acquired from Landsat 8 images during the tomato crop cycle varied according to the development stage and cultivated area.

ET_a values were more uniform throughout the areas studied by the SAFER than the METRIC algorithm, suggesting higher reliability in the SAFER model.

ET_{SAFER} and ET_{METRIC} values were lower in all areas at the beginning of the cycle with little vegetation cover, during seedling establishment, at the end of the cycle when tomato plants begin the senescence stage, and at the beginning of harvesting compared with the vegetative and fructification phases of tomato crops for industrial processing. The METRIC algorithm values were lower than SAFER for these low evapotranspiration phases.

The no-till farming areas presented a lower discrepancy in evapotranspiration values during the beginning of the cycle with the standard methods than conventional farming areas. Adequate amounts of straw covering the soil alters the soil-water-atmosphere relationship, especially at the start of the cycle, when the crop's leaf area index does not entirely cover the soil (Warreen et al. 2014).

Xue et al. (2020) measured the ET_a of tomato crops for industrial processing using orbital images, noting the underestimation of ET_{METRIC} at the beginning of the cycle. The same authors attributed this behavior to the influence of exposed soil and the underestimated average net radiation when empirical equations measure it by resizing instantaneous evapotranspiration for ET_a.

In another perspective, low evapotranspiration values at the beginning of the crop cycle may occur because K_c varies with high water evaporation.

SAFER and METRIC models usually estimate higher evapotranspiration values during the vegetative phase (flowering onset) and the beginning of fructification. Maximum ET_{SAFER} and ET_{METRIC} values were 5.2 mm and 5.0 mm d^{-1} (Figure 2.6), respectively, corresponding to the crop period with higher vigor - the vegetative stage of fructification.

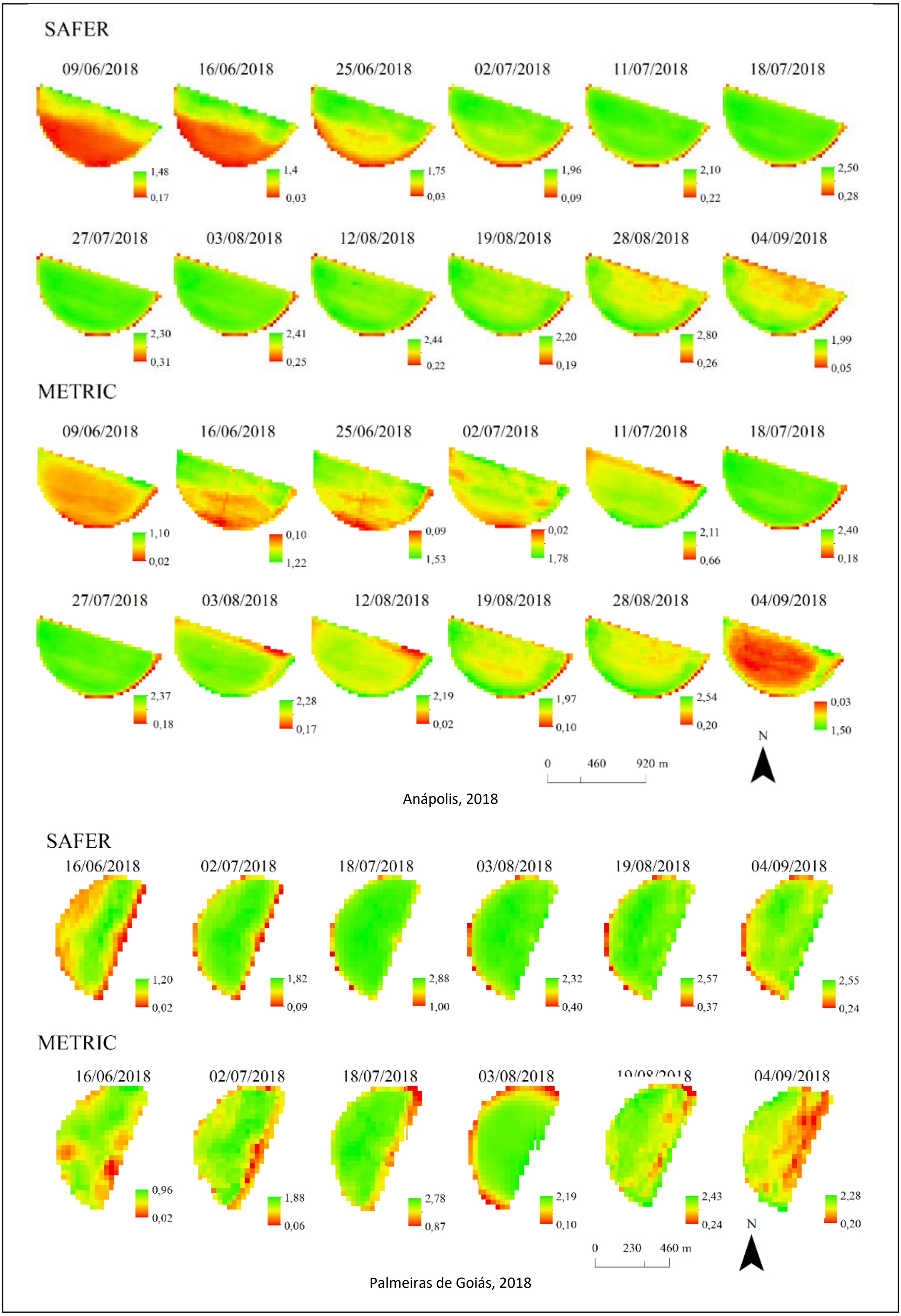

Figure 2. Spatiotemporal distribution of evapotranspiration for tomato crops for industrial processing measured by the SAFER (ET_{SAFER}) and METRIC (ET_{METRIC}) models in Anápolis-GO and Palmeiras de Goiás-GO, in 2018.

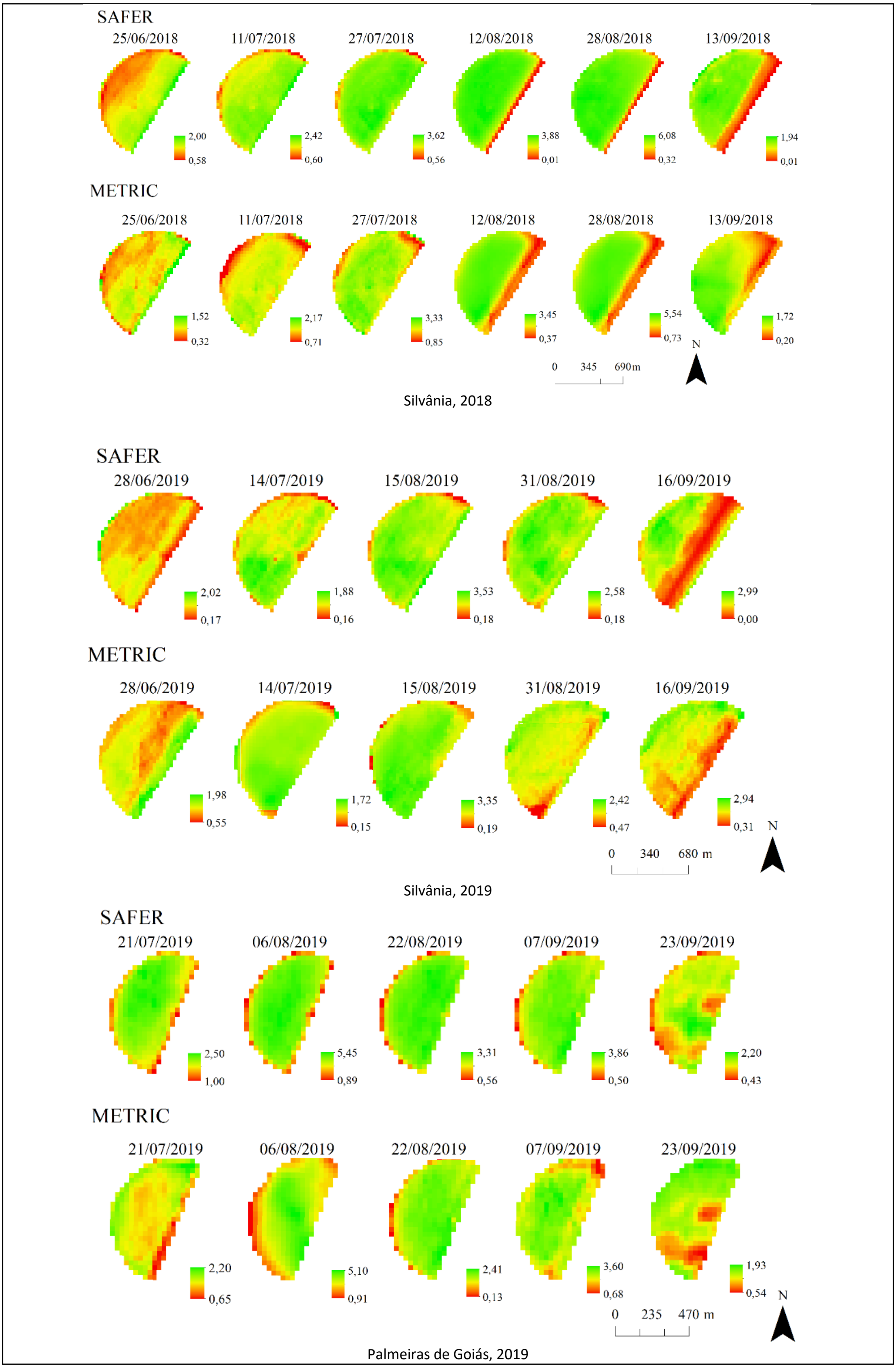

Figure 3. Spatiotemporal distribution of evapotranspiration for tomato crops for industrial processing measured by the SAFER (ET_{SAFER}) and METRIC (ET_{METRIC}) models in Silvânia-GO, in 2018, and Silvânia and Palmeiras de Goiás-GO in 2019.

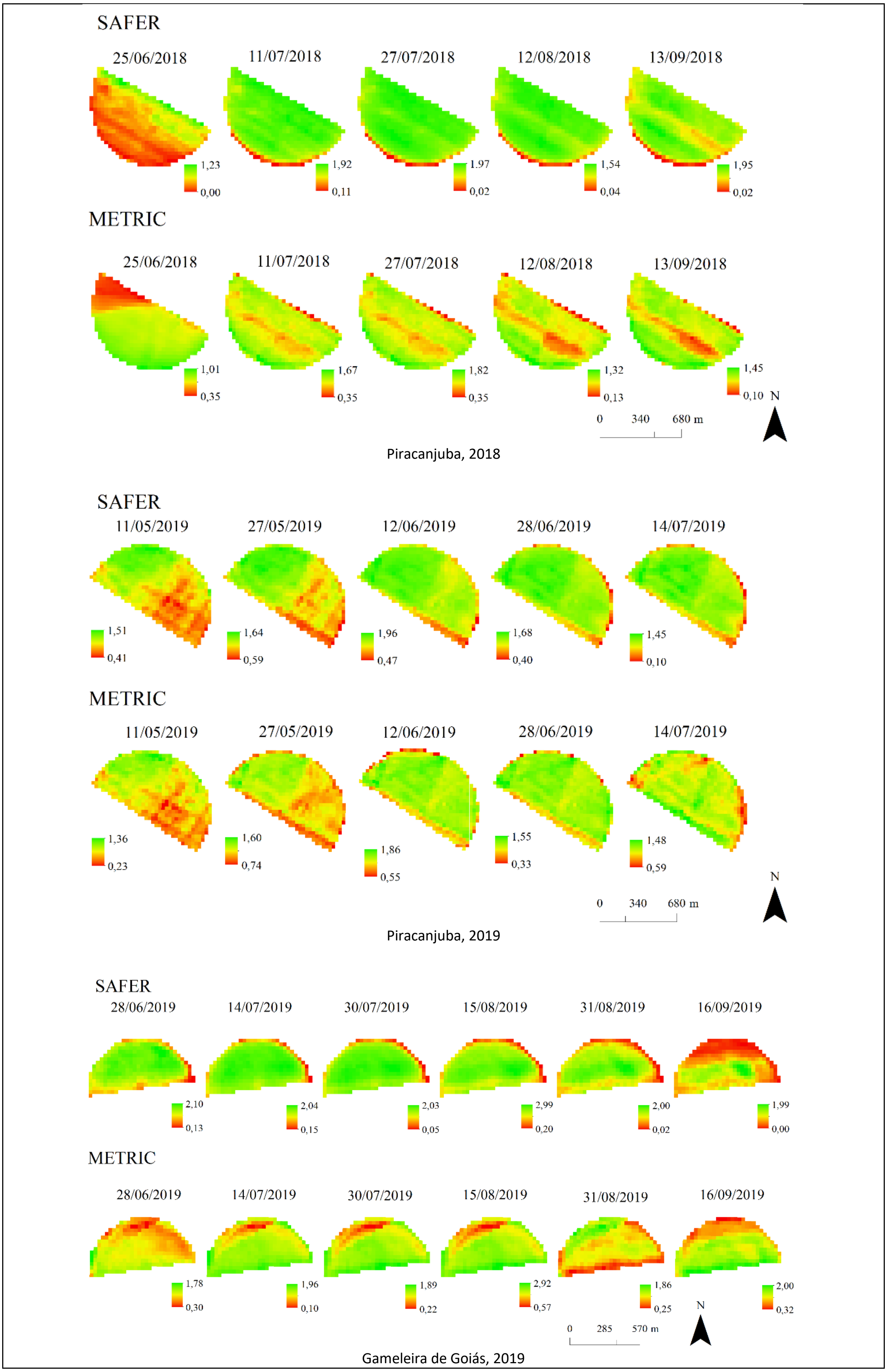

Figure 4. Spatiotemporal distribution of evapotranspiration for tomato crops for industrial processing measured by the SAFER (ET_{SAFER}) and METRIC (ET_{METRIC}) models in Piracanjuba-GO in 2018/2019, and in Gameleira de Goiás-GO in 2019.

Despite their similarities, the data of phases II and III of tomato crops for industrial processing showed lower ET_{METRIC} and ET_{SAFER} values than ET_{BHS}, ET_{FAO}, and $ET_{Embrapa}$.

The most significant differences for ET_a measured by the SAFER model were 0.48 mm d^{-1} compared with $ET_{Embrapa}$, 0.68 mm d^{-1} compared with $ET_{FAO,}$ and 0.85 mm d^{-1} compared with ET_{BHS}. As for the METRIC model, ET_a differences were 0.77, 2.08 and 1.53 mm d^{-1} compared with $ET_{Embrapa}$, $ET_{FAO,}$ and ET_{BHS}, respectively. In both cases, the algorithms underestimated crop evapotranspiration (ET_c).

Tables 3, 4 and 5 present statistical indices for estimating ET_{SAFER} and ET_{METRIC} values compared with FAO, Embrapa, and BHS methods, respectively. The findings indicate that SAFER and METRIC can estimate the evapotranspiration of tomato crops for industrial processing, as they show good correction, agreement, and low error.

Table 3. Statistical analysis for evapotranspiration values obtained by the SAFER and METRIC models compared with ET_{FAO}.

Location	Model	MSE	MAE	d
Anápolis – 2018	SAFER	0.088	0.262	0.88
	METRIC	0.279	0.431	0.72
Palmeiras de Goiás – 2018	SAFER	0.165	0.308	0.83
	METRIC	0.331	0.455	0.71
Palmeiras de Goiás – 2019	SAFER	0.388	0.324	0.86
	METRIC	0.716	0.536	0.74
Silvânia – 2018	SAFER	0.452	0.337	0.87
	METRIC	0.621	0.453	0.82
Silvânia – 2019	SAFER	0.586	0.541	0.64
	METRIC	0.730	0.611	0.57
Piracanjuba – 2018	SAFER	0.063	0.156	0.91
	METRIC	0.134	0.234	0.83
Piracanjuba – 2019	SAFER	0.033	0.113	0.92
	METRIC	0.061	0.165	0.88
Gameleira de Goiás – 2019	SAFER	0.157	0.212	0.76
	METRIC	0.235	0.318	0.72

MSE = Mean squared error (mm d^{-1}); MAE = mean absolute error (mm d^{-1}); r = correlation coefficient; d = index of agreement.

Table 4. Statistical analysis for evapotranspiration values obtained by the SAFER and METRIC models compared with $ET_{Embrapa}$.

Location	Model	MSE	MAE	d
Anápolis – 2018	SAFER	0.021	0.113	0.97
	METRIC	0.081	0.252	0.90
Palmeiras de Goiás – 2018	SAFER	0.011	0.057	0.99
	METRIC	0.049	0.161	0.95
Palmeiras de Goiás – 2019	SAFER	0.008	0.059	1.00
	METRIC	0.136	0.264	0.96
Silvânia – 2018	SAFER	0.054	0.163	0.99
	METRIC	0.148	0.280	0.96
Silvânia – 2019	SAFER	0.030	0.081	0.98
	METRIC	0.068	0.144	0.94
Piracanjuba – 2018	SAFER	0.013	0.061	0.98
	METRIC	0.038	0.139	0.94
Piracanjuba – 2019	SAFER	0.008	0.058	0.98
	METRIC	0.016	0.085	0.97
Gameleira de Goiás – 2019	SAFER	0.012	0.052	0.97
	METRIC	0.056	0.158	0.91

MSE = Mean squared error (mm d^{-1}); MAE = mean absolute error (mm d^{-1}); r = correlation coefficient; d = index of agreement.

Table 5. Statistical analysis for evapotranspiration values obtained by the SAFER and METRIC models compared with ET_{BHS}.

Location	Model	MSE	MAE	d
Anápolis – 2018	SAFER	0.055	0.153	0.89
	METRIC	0.172	0.330	0.74
Palmeiras de Goiás – 2018	SAFER	0.124	0.277	0.86
	METRIC	0.222	0.423	0.78
Palmeiras de Goiás -2019	SAFER	0.179	0.211	0.93
	METRIC	0.431	0.426	0.84
Silvânia – 2018	SAFER	0.052	0.161	0.99
	METRIC	0.132	0.256	0.96
Silvânia – 2019	SAFER	0.210	0.334	0.77
	METRIC	0.287	0.404	0.67
Piracanjuba – 2018	SAFER	0.111	0.249	0.83
	METRIC	0.185	0.326	0.76
Piracanjuba – 2019	SAFER	0.010	0.076	0.98
	METRIC	0.029	0.129	0.95
Gameleira de Goiás – 2019	SAFER	0.040	0.134	0.92
	METRIC	0.087	0.209	0.87

MSE = Mean squared error (mm d^{-1}); MAE = mean absolute error (mm d^{-1}); r = correlation coefficient; d = index of agreement.

ET_{SAFER} and ET_{METRIC} correlated better overall with $ET_{Embrapa}$ than with ET_{BHS} and ET_{FAO}. The SAFER model showed MSE values between 0.01 mm and 0.59 mm d^{-1}, 0.02 mm d^{-1} compared with $ET_{Embrapa}$, 0.24 compared with ET_{FAO}, and 0.09 mm d^{-1} compared with ET_{BHS}. The MAE for the analyzed areas were lower than 1, 0.008 mm d^{-1} compared with $ET_{Embrapa}$, 0.28 mm d^{-1} compared with ET_{FAO}, and 0.19 mm d^{-1} compared with ET_{BHS}.

The METRIC model also satisfactorily estimated the ET_a of tomato crops for industrial processing, with a maximum MSE of 0.73 mm d^{-1} and MAE of 0.61 mm d^{-1} for the analyzed areas. The low ET_a values at the beginning and end of the cycle (as mentioned for the studied models) increased MSE, MAE, and the statistical coefficients compared with ET_{FAO}, as the initial and final K_c used in this method are inadequate for this study area.

The "d" index of agreement varied between 0.64 and 0.99 for SAFER and 0.57 and 0.97 for METRIC. Both algorithms presented a lower index of agreement for the cultivated area in Silvânia in 2018.

The correlation coefficient (r) and the confidence index (c) also confirmed the algorithms' satisfactory performance in measuring the ET_a of tomato crops for industrial processing.

One disadvantage of using satellite images in agriculture is their limitation regarding the revisit frequency within the crop cycle and the interference from clouds in imaging analyses. Thus, the fewer images (samples) may decrease the models' precision and accuracy of evapotranspiration measurements.

The low MSE and MAE values confirm the high r values and demonstrate a high linear statistical dependence between the analyzed variables and the high coefficient of determination (R^2) (Figure 5).

The performance of SAFER and METRIC algorithms regarding the growth stages of processing tomato demonstrate that the vegetative (Phase II) and fructification (Phase III) stages present higher analogies of ET_{SAFER} and ET_{METRIC} with ET_c estimated by BHS, FAO, and Embrapa (Figure 6). The coefficient of determination considering both evapotranspiration estimation models obtained overall means of 0.67, 0.89, 0.96, and 0.58 for Phases I, II, III, and IV, respectively.

In phase I, the METRIC model presented a lower MSE of 0.136 mm d^{-1}, MAE of 0.292 mm d^{-1}, and d of 0.74, classifying it as "sufferable" (Table 6). In phase II, SAFER presented minimum MSE and MAE values of 0.046 and 0.142 mm d^{-1}, respectively.

Regarding phases II and III, the correlation coefficients and indices of agreement varied between 0.89 and 0.99. The SAFER and METRIC models in phase IV showed indices of agreement between 0.52 and 0.95. That confirms that the algorithms did not accurately measure evapotranspiration at the beginning and end of the tomato crop cycle, thus underestimating such value.

The SAFER model performed better than the METRIC model in measuring ET_a. The ET_{METRIC} values were lower than the ET_a values measured by SAFER, which, in turn, underestimated the $ET_{Embrapa}$, $ET_{FAO,}$ and

ET_{BHS} results. One of the main differences between the algorithms is that METRIC requires "anchor" pixels in the same area with extreme thermo-hydrological conditions to measure ET_a, thus limiting its application.

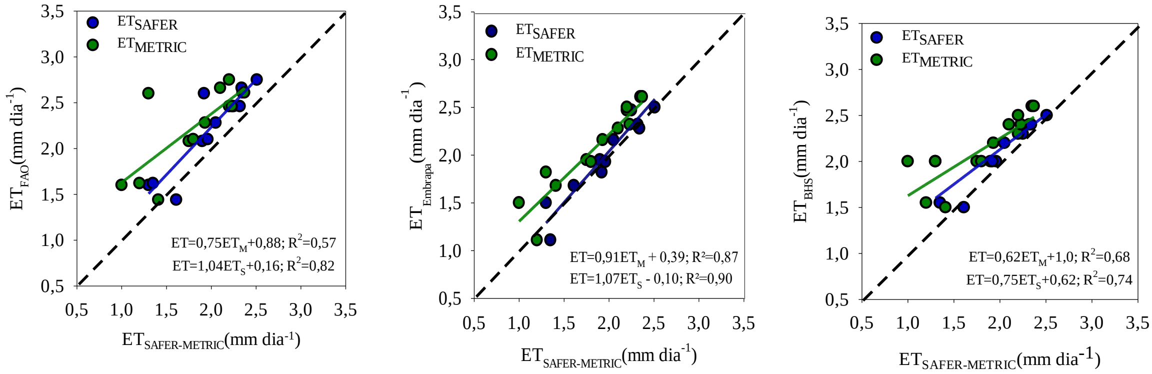

Anápolis - 2018

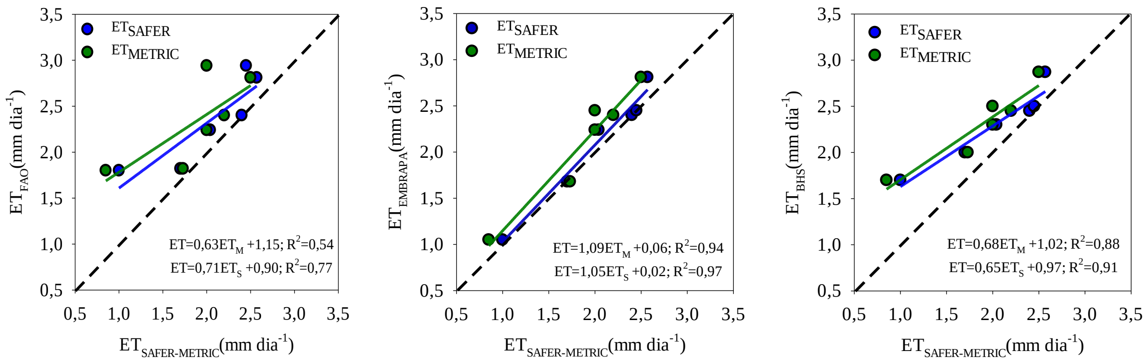

Palmeiras de Goiás - 2018

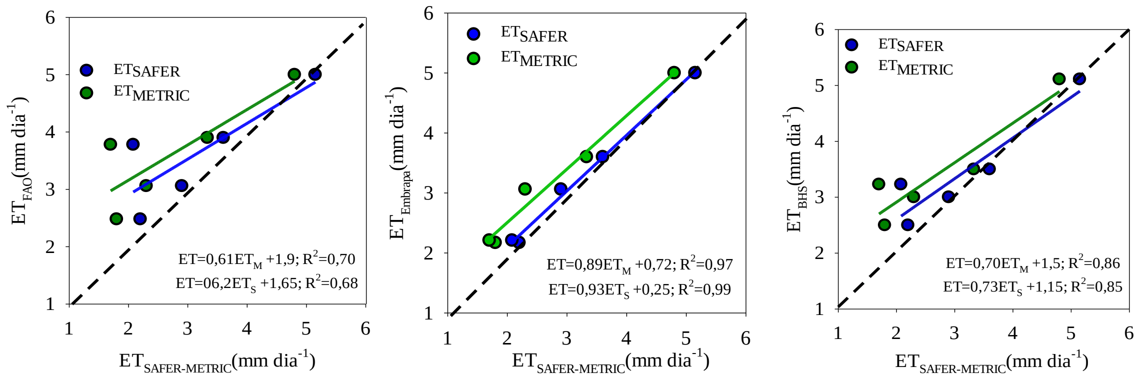

Palmeiras de Goiás - 2019

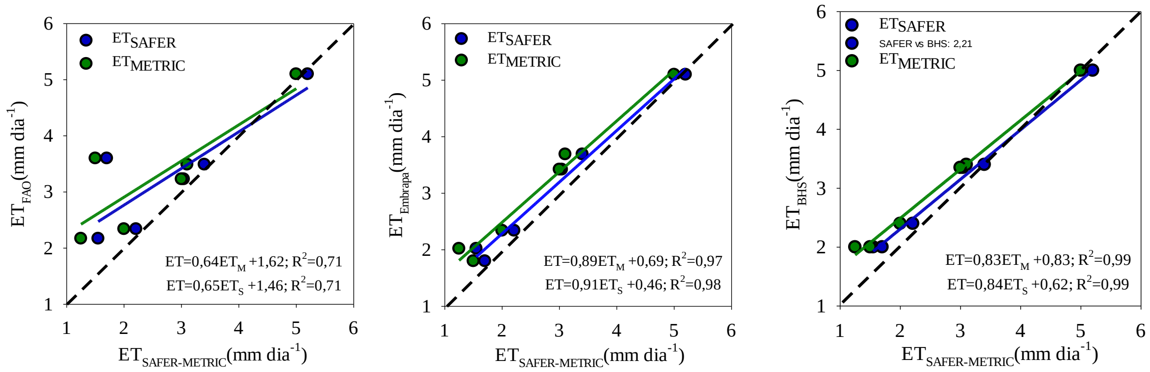

Silvânia – 2018

Figure 5. Continued.

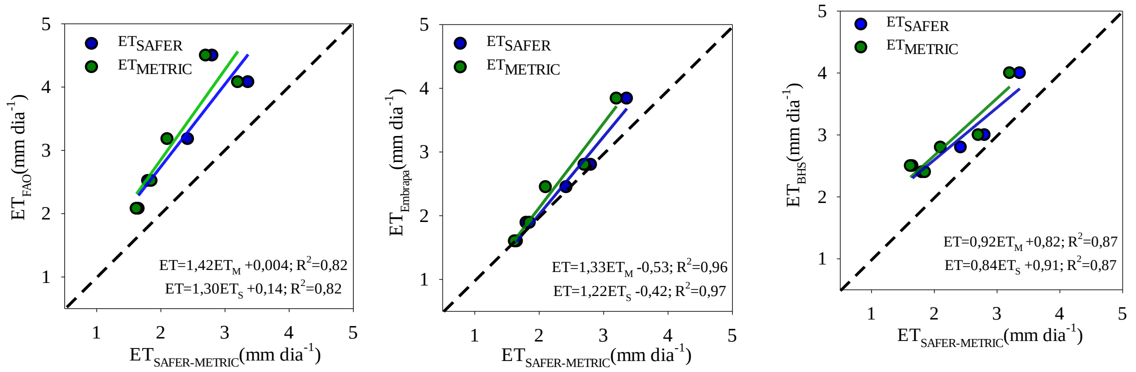

Silvânia - 2019

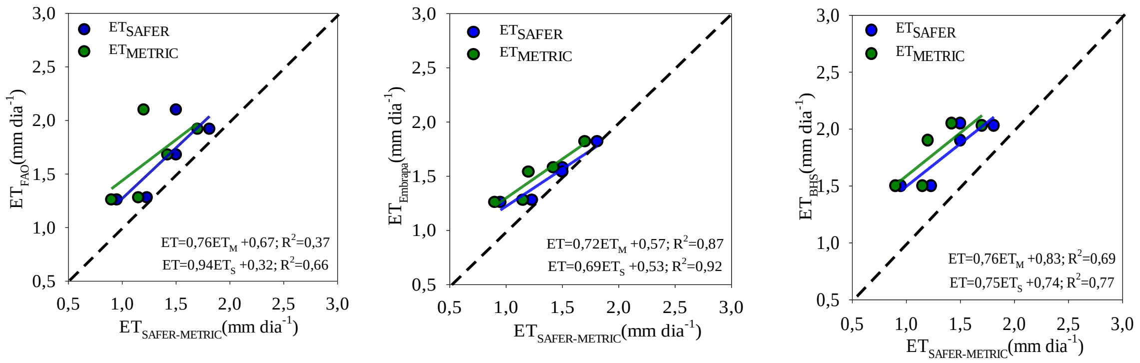

Piracanjuba - 2018

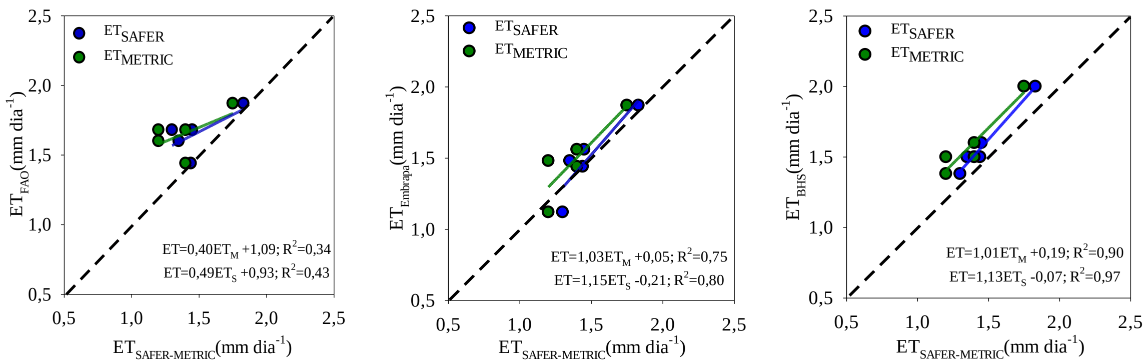

Piracanjuba - 2019

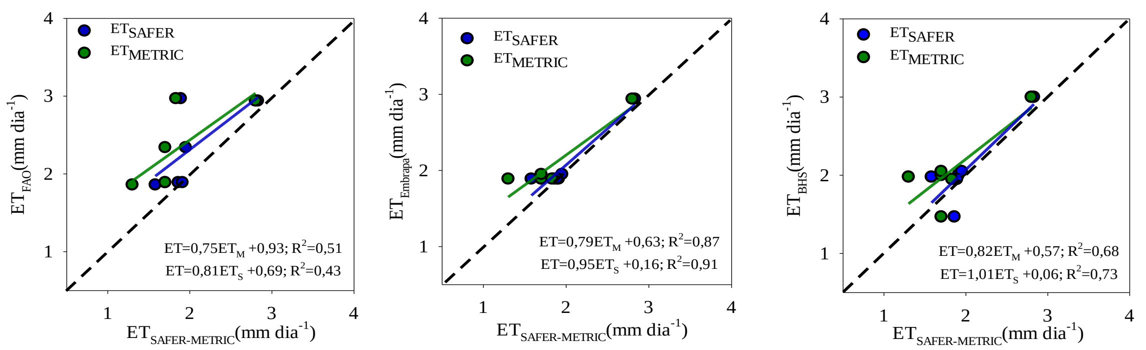

Gameleira de Goiás -2019

Figure 5. Straight line 1:1 comparing the evapotranspiration measured by SAFER (ET_{SAFER}) and METRIC (ET_{METRIC}) models with FAO (ET_{FAO}), Embrapa ($ET_{Embrapa}$), and soil water balance (ET_{BHS}) standard methods.

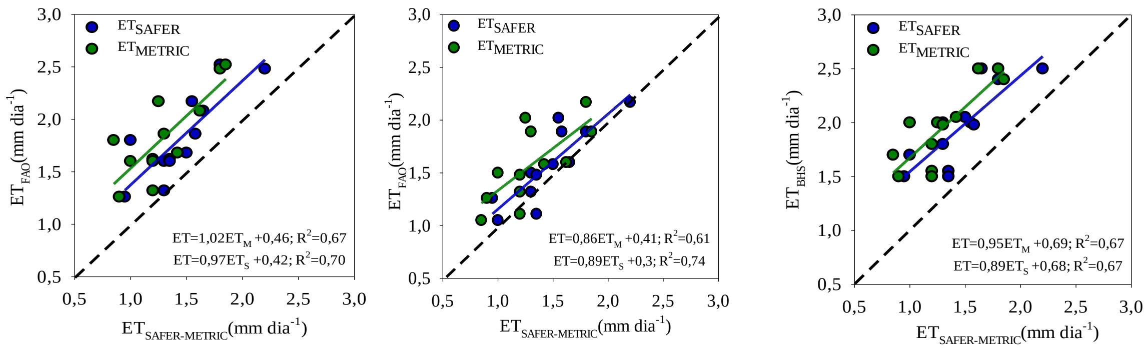

Phase I

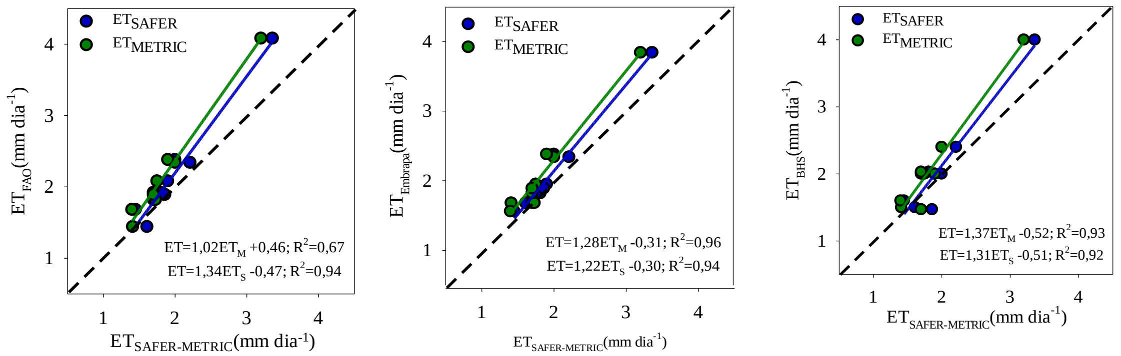

Phase II

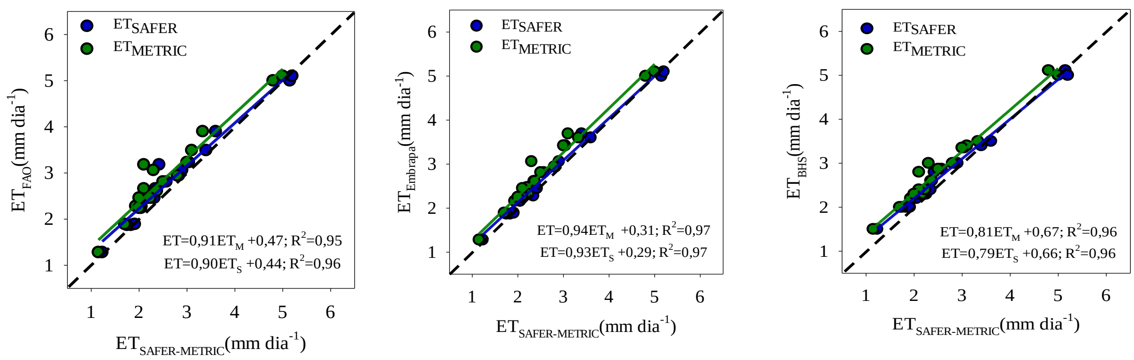

Phase III

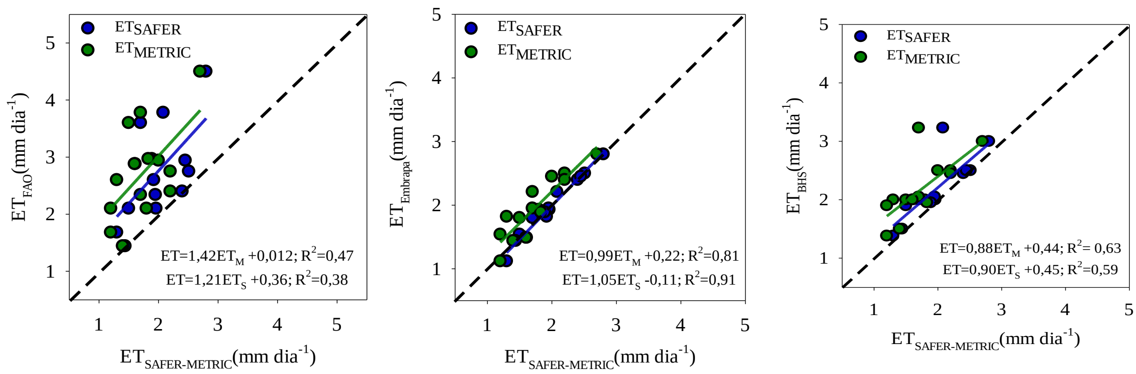

Phase IV

Figure 6. Straight line 1:1 comparing the evapotranspiration measured by SAFER (ET_{SAFER}) and METRIC (ET_{METRIC}) models with FAO (ET_{FAO}), Embrapa ($ET_{Embrapa}$), and soil water balance (ET_{BHS}) standard methods regarding the development phases of tomato plants.

Table 6. Statistical analysis for evapotranspiration by the SAFER and METRIC models compared with the ET_{FAO}, $ET_{Embrapa}$, and ET_{BHS} methods regarding the development phases.

Model		MSE	MAE	d
		Phase I		
SAFER	FAO	0.187	0.372	0.72
	Embrapa	0.046	0.165	0.89
	BHS	0.286	0.496	0.63
METRIC	FAO	0.341	0.533	0.58
	Embrapa	0.136	0.292	0.74
	BHS	0.470	0.658	0.52
		Phase II		
SAFER	FAO	0.091	0.230	0.94
	Embrapa	0.046	0.142	0.97
	BHS	0.087	0.233	0.94
METRIC	FAO	0.156	0.316	0.91
	Embrapa	0.105	0.272	0.93
	BHS	0.128	0.297	0.92
		Phase III		
SAFER	FAO	0.068	0.207	0.98
	Embrapa	0.029	0.135	0.99
	BHS	0.039	0.167	0.99
METRIC	FAO	0.178	0.345	0.95
	Embrapa	0.099	0.267	0.97
	BHS	0.116	0.298	0.97
		Phase IV		
SAFER	FAO	0.972	0.755	0.59
	Embrapa	0.006	0.051	0.95
	BHS	0.129	0.212	0.85
METRIC	FAO	1.384	0.982	0.53
	Embrapa	0.084	0.242	0.89
	BHS	0.317	0.438	0.70

MSE = Mean squared error (mm d^{-1}); MAE = mean absolute error (mm d^{-1}); r = correlation coefficient; d = index of agreement.

4. Discussion

This study verified an ability to simulate the spatial variability of evapotranspiration (ET) during a cycle in a given area based on other studies using SAFER (Santos et al. 2020; Mussi et al. 2020) and METRIC (Poças et al. 2014; Khand et al. 2017; Oliveira et al. 2018) algorithms.

Teixeira et al. (2013) also reported uniformity in actual evapotranspiration (ET_a) values across scientific areas by the SAFER algorithm compared to METRIC while verifying the application of the SAFER and SEBAL algorithms. The authors also found that SEBAL presented this alteration to measure ET.

ET_{SAFER} and ET_{METRIC} values at the start of the cycle and harvesting are often the lowest when measuring crops' ET using satellite images (French et al. 2015; Sales et al. 2016; Sales et al. 2017; Althoff et al. 2019; Souza et al. 2020). That may be due to exposed soil at the beginning and end of the cycle, which interferes with the determination of vegetation indices (NDVI, SAVI, and IAF), one of the input factors for measuring ET by remote sensing (Filgueiras et al. 2019; Venancio et al. 2020; Venancio et al. 2021).

No-tillage areas present lower ET discrepancies at the beginning of the cycle than those with conventional cultivation. That is because adequate amounts of straw covering the soil alters the soil-water-atmosphere relationship, especially at the start of the cycle when the crop's leaf area index does not entirely cover the soil (Warreen et al. 2014).

ET_{SAFER} and ET_{METRIC} remained relatively high and uniform until the end of this phase due to the crop establishment in the area, also reported by Teixeira et al. (2013).

Marouelli et al. (2012) found that crop evapotranspiration (ET_c) increases in phases with more vegetative development and decreases until the tomato's physiological maturation phase. High evapotranspiration values measured by satellite images were found in the fructification phase of corn crops (Althoff et al. 2019; Santos et al. 2020) and the fully developed phase in sugar cane (Mussi et al. 2020) and common bean (Sales et al. 2017) crops.

ET_{METRIC} and ET_{SAFER} values during phases II and III of tomato cultivation for industrial processing were lower than ET_{BHS}, ET_{FAO}, and $ET_{Embrapa}$ values. Sales et al. (2017) reported a similar result for tomato crops for industrial processing using the SAFER algorithm.

ET_a values were low at the beginning and end of the cycle for the analyzed models, making the initial and final single crop coefficient (K_c) misleading. Liu et al. (2019) also described that measuring evapotranspiration in crop extremes interferes with a model's relative error.

Reyes-Gonzáles et al. (2020) compared ET_a in corn crops measured by METRIC with ET_a determined by an actinometer, finding a difference of 1.4 mm d^{-1}. They attributed this variation mainly to the high wind speed when the satellite passed over the area and the satellite's underestimation of this influence while determining ET. Nevertheless, METRIC demonstrated good agreement and a high coefficient of determination while measuring ET_a.

The SAFER algorithm also presented satisfying statistical results for estimating the ET of sugar cane (Mussi et al. 2020; Souza et al. 2020), common bean (Sales et al. 2016), corn (Althoff et al. 2019), and tomato for industrial processing, with errors lower than 1 mm d^{-1} (Sales et al. 2017). Thus, SAFER may be applied to different cultures.

SAFER seemed promising for measuring the ET_a of tomato crops, presenting sensibility to variations in tomato plant conditions. This method provides variations over time and a low cost to obtain information, potentially aiding irrigation management (Souza et al. 2020) without discarding the need for meteorological stations close to the areas of interest and equation parameter adjustments (Teixeira et al. 2013).

However, the cultivated area may not have extreme pixels due to the unwanted incidence of exposed soil or, conversely, when hot pixels are not easily located after irrigation (Jaafar and Ahmad 2020) or when the analyzed areas are small and homogeneous. The presented extreme pixels (cold and hot) may be invalid (Xue et al. 2020).

Nevertheless, the SAFER model requires the "a" and "b" regression coefficients to recover ET_a, as recommended by Teixeira et al. (2013). These empirical coefficients may decrease algorithm efficiency, potentially varying according to the region and soil use. Venancio et al. (2021) applied the SAFER algorithm with coefficients of 1.8 and 0.008, verifying weak performance in measuring ET in irrigated corn crops in the Brazilian semiarid region. Still, the calibration of new coefficients (a = 0.32 and b = - 0.0013) enhanced algorithm performance for ET measurement.

5. Conclusions

The SAFER and METRIC algorithms can measure the ET_a of tomato crops for industrial processing with center-pivot irrigation in south-central regions of Goiás. These algorithms were more accurate than FAO, BHS, and Embrapa methods to measure ET_c. The SAFER and METRIC models showed a lower mean absolute error of 0.24 mm d^{-1} in the vegetative and fructification phases. SAFER presented better statistical performance than METRIC; however, both underestimated the evapotranspiration of tomato crops for industrial processing.

Authors' Contributions: SENA, C.C.R.: Conceptualization, research planning, methodology, field data collection and tabulation, statistical analysis, writing of the discussion and results, scientific writing, supervision; ALVES JUNIOR, J.: Conceptualization, research planning, methodology, Writing of the discussion and results, supervision; SOUZA, J.M.F.: conceptualization, methodology, writing of the discussion and results,; CASAROLI, D.: methodology, scientific writhing; BATTISTI, R.: methodology, statistical analysis, scientific writing; ANTUNES JUNIOR, E.J.: methodology, field data collection and tabulation, statical analysis; EVANGELISTA, A.W.P.: writing of the discussion and results, scientific writing.

Conflicts of Interest: The authors declare no conflicts of interest.

Ethics Approval: Not applicable.

Acknowledgments: The research is also part of Carolina Sena's PhD. The authors would like to thank Federal University of Goiás (UFG) and Foundation for Research Support of the State of Goiás (FAPEG) and the Coordination for the Improvement of Higher Education Persons (CAPES) for support.

References

ALLEN, R.G., et al. Satellite-based ET estimation in agriculture using SEBAL and METRIC. *Hydrological Process*. 2011, **25**, 4011-4027. https://doi.org/10.1002/hyp.8408

ALLEN R.G., et al. Crop evapotranspiration: Guidelines for computing crop water requirements. FAO Irrigation and drainage paper No. 56. FAO. Rome, Italy; 1998, **300**(9). Available from: http://www.fao.org/tempref/SD/Reserved/Agromet/PET/FAO_Irrigation_Drainage_Paper_56.pdf

ALLEN, R.G., et al. Satellite-based energy balance for mapping evapotranspiration with internalized calibration (METRIC)-Applications. *Journal of Irrigation and Drainage Engineering*. 2007, **133**(4), 395-406. https://doi.org/10.1061/(ASCE)0733-9437(2007)133

ALLEN R.G., et al. A Landsat-based energy balance and evapotranspiration model in Western US water rights regulation and planning. *Irrigation and Drain System*. 2005, **19**(3-4), 251-268. https://doi.org/10.1007/s10795-005-5187-z

ALTHOFF, F., et al. Evapotranspiration for irrigated agriculture using orbital satellites. *Bioscience Journal*. 2019, **35**(3), 670-678. https://doi.org/10.14393/BJ-v35n3a2019-41737

BASÍLIO, E.E., et al. Intervalos de irrigação no cultivo de tomateiro para processamento. *Irriga*. 2019, **24**(4), 676-692. https://doi.org/10.15809/irriga.2019v24n4p676-692

BASTIAANSSEN, W.G.M., et al. A remote sensing surface energy balance algorithm for land (SEBAL): 1. Formulation. *Journal of Hydrology*. 1998, **212-213**, 198-212. https://doi.org/10.1016/S0022-1694(98)00253-4

BREKSA, A.P., et al. Physicochemical and morphological analysis of ten tomato varieties identifies quality traits more readily manipulated through breeding and traditional selection methods. *Journal of Food Composition and Analysis*. 2015, **42**, 16-25. https://doi.org/10.1016/j.jfca.2015.02.011

CARDOSO, M.R.D., MARCUZZO, F.F.N. e BARROS, J.R. Classificação climática de Köppen-Geiger para o estado de Goiás e o Distrito Federal. *Acta Geográfica*. 2014, **8**(16) 40-55. http://dx.doi.org/10.5654/acta.v8i16.1384

DIAS, S.H.B., et al. Reference evapotranspiration of Brazil modeled with machine learning techniques and remote sensing. *Plos one*. 2021, **16**(2), e0245834. https://doi.org/10.1371/journal.pone.0245834

ELKATOURY, A., ALAZBA, A.A. e MOSSAD, A. Estimating Evapotranspiration Using Coupled Remote Sensing and Three SEB Models in an Arid Region. *Environmental Processes*. 2019, **7**(1), 109-133. https://doi.org/10.1007/s40710-019-00410-w

EMPRESA BRASILEIRA DE PESQUISA AGROPECUÁRIA – EMBRAPA. Centro Nacional de Pesquisa de Solos. Sistema brasileiro de classificação de solos. 3.ed. Brasília, Produção de Informação. 353p, 2013. Available from: https://www.embrapa.br/solos/sibcs

FILGUEIRAS, R., et al. Sensitivity of evapotranspiration estimated by orbital images under influence of surface temperature, *Engenharia Agrícola*. 2019, **39**, 23-32. http://dx.doi.org/10.1590/1809-4430-eng.agric.v39nep23-32/2019.

FRENCH, A.N., HUNSAKER, D.J. e THORP, K.R. Remote sensing of evapotranspiration over cotton using the TSEB and METRIC energy balance models. *Remote Sensing of Environment*. 2015, **158**, 281-294. https://doi.org/10.1016/j.rse.2014.11.003

HERNANDEZ, F.B.T., et al. Determining large scale actual evapotranspiration using agrometeorological and remote sensing data in the Northwest of Sao Paulo State, Brazil. *Acta Horticulturae*. 2014, **1038**, 263-270. https://doi.org/10.17660/ActaHortic.2014.1038.31

INSTITUTO BRASILEIRO DE GEOGRAFIA E ESTATÍSTICA – IBGE. Levantamento Sistemático da Produção Agrícola, 2019. Available from: https://biblioteca.ibge.gov.br/visualizacao/periodicos/2415/epag_2019_jan.pdf

JAAFAR, H.H. e AHMAD, F.A. Time series trends of Landsat-based ET using automated calibration in METRIC and SEBAL: The Bekaa Valley, Lebanon. *Remote Sensing of Environment*. 2020, **238**, 111034. https://doi.org/10.1016/j.rse.2018.12.033

KHAND, K., KJAERSGAARD, J., HAY, C. e JIA, X. Estimating Impacts of Agricultural Subsurface Drainage on Evapotranspiration Using the Landsat Imagery - Based METRIC Model. *Hydrology*. 2017, **4**(4), 29. https://doi.org/10.3390/hydrology4040049

KHAND, K., et al. Dry Season Evapotranspiration Dynamics over Human-Impacted Landscapes in the Southern Amazon Using the Landsat-Based METRIC Model. *Remote Sensing*. 2017, **9**(7), 706. https://doi.org/10.3390/rs9070706

KOTTEK, M., et al. World Map of the Köppen-Ginger climate classification update. *Meteorologische Zeitschrift*. 2006, **15**(3), 259-263. https://doi.org/10.1127/0941-2948/2006/0130

LIBARDI, P.L. Dinâmica da água no solo. 2. ed. São Paulo: Universidade de São Paulo; 352 p, 2012.

LIU, R., et al. Actual daily evapotranspiration estimated from MERIS and AATSR data over the Chinese Loess Plateau. *Hydrology and Earth System Sciences*. 2010, **14**(1), 47-58. https://doi.org/10.5194/hess-14-47-2010

MAROUELLI, W.A., SILVA, H.R. e SILVA, W.L.C. Irrigação do tomateiro para processamento. Brasília: Embrapa Hortaliças, Circular técnica 102, p. 24, 2012. Available from: https://www.infoteca.cnptia.embrapa.br/infoteca/bitstream/doc/925502/1/1113CT102Prova20120312.pdf

MAROUELLI, W.A. e SILVA, W.L.C. Irrigação por gotejamento do tomateiro industrial durante o estádio de frutificação, na região do cerrado. *Horticultura Brasileira*. 2006, **24**(3), 342-346. https://doi.org/10.1590/S0102-05362006000300014

MUSSI, R.F.M., et al. Evapotranspiração da cana-de-açúcar estimada pelo algoritmo SAFER. *Irriga*. 2020, **25**(2), 263-278. https://doi.org/10.15809/irriga.2020v25n2p263-278

NORMAN, J.M. e BECKER, F. Terminology in thermal infrared remote sensing of natural surfaces. *Agricultural and Forest Meteorology*. 1995, **77**(3-4), 153-166. https://doi.org/10.1016/0168-1923(95)02259-Z

OLIVEIRA, B.S., et al. Improved Albedo Estimates Implemented in the METRIC Model for Modeling Energy Balance Fluxes and Evapotranspiration over Agricultural and Natural Areas in the Brazilian Cerrado. *Remote Sensing*. 2018, **10**(8), 1181. https://doi.org/10.3390/rs10081181

PETROPOULOS, G.P., et al. Earth Observation-Based Operational Estimation of Soil Moisture and Evapotranspiration for Agricultural Crops in Support of Sustainable Water Management. *Sustainability*. 2018, **10**(1), 181. https://doi.org/10.3390/su10010181

PIRES, G.F., et al. Increased climate risk in Brazilian double cropping agriculture systems: implications for land use in Northern Brazil. *Agricultural and Forest Meteorology*. 2016, **228**, 286-298. https://doi.org/10.1016/j.agrformet.2016.07.005

POÇAS, I., et al. Satellite-based evapotranspiration of a super-intensive olive orchard: Application of METRIC algorithms. *Biosystems engineering*. 2014, **128**, 69-81. https://doi.org/10.1016/j.biosystemseng.2014.06.019

REYES-GONZÁLEZ, A., et al. Comparison of Leaf Area Index, Surface Temperature, and Actual Evapotranspiration Estimated Using the METRIC Model and In Situ Measurements. *Sensors*. 2019, **19**(8), 1857. https://doi.org/10.3390/s19081857

SACCON, P. Water for agriculture, irrigation management. *Applied Soil Ecology*. 2018, **123**, 793-796. https://doi.org/10.1016/j.apsoil.2017.10.037

SALES, D.L.A., et al. Estimativa de evapotranspiração e coeficiente de cultura do tomateiro industrial utilizando o algoritmo SAFER. *Irriga*. 2017, **22**(3), 629-640. https://doi.org/10.15809/irriga.2017v22n3p629-640

SALES, D.L.A., et al. Common bean evapotranspiration estimated by orbital images. African *Journal of Agricultural Research*. 2016, **11**, 867-872. https://doi.org/10.5897/AJAR2015.10500

SANTOS, R.A., et al. Remote sensing as a tool to determine biophysical parameters of irrigated seed corn crop. *Semina: Ciências Agrárias*. 2020, **41**(2), 435-446. http://dx.doi.org/10.33/1679-0359.2020v41n2p435

SENA, C.R.S., et al. Calibração do sensor capacitivo de umidade do solo EC-5 em resposta a granulometria do solo. *Brazilian Journal of Development*. 2020, **6**(4), 17228-17240. https://doi.org/10.34117/bjdv6n4-043

SENAY, G.B., et al. Evaluating Landsat 8 evapotranspiration for water use mapping in the Colorado River Basin. *Remote Sensing of Environment*. 2016, **185**(3), 171-185. https://doi.org/10.1016/j.rse.2015.12.043

SINGH, A. Assessment of different strategies for managing the water resources problems of irrigated agriculture, *Agricultural Water Management*. 2018, **208**, 187-192. https://doi.org/10.1016/j.agwat.2018.06.021

SINGH, A. Managing the water resources problems of irrigated agriculture through geospatial techniques: An overview. *Agricultural Water Management*. 2016, **174**, 2-10. https://doi.org/10.1016/j.agwat.2016.04.021

SOUZA, J.M.F., et al. Validação do modelo SAFER na estimativa da evapotranspiração da cana-de-açúcar. *Irriga*. 2020, **25**(2), 247-262. https://doi.org/10.15809/irriga.2020v25n2p247-262

TEIXEIRA, A.H.C., et al. Modelagem espaço temporal dos componentes dos balanços de energia e de água no Semiárido brasileiro. Embrapa Monitoramento por Satélite Campinas, SP. Documentos, 99, 2013. Available from: https://ainfo.cnptia.embrapa.br/digital/bitstream/item/93401/1/Bassoi-2013.pdf

TEIXEIRA, A.H.C., et al. Large-scale radiation and energy balances with Landsat 8 images and agrometeorological data in the Brazilian semiarid region. *Journal of Applied Remote Sensing*. 2017, **11**(1), 016030. https://doi.org/10.1117/1.JRS.11.016030

TEIXEIRA, A.H.C. Determining regional actual evapotranspiration of irrigated and natural vegetation in the São Francisco river basin (Brazil) using remote sensing an Penman-Monteith equation. *Remote Sensing*. 2010, **2**(5), 1287-1319. https://doi.org/10.3390/rs0251287

TEIXEIRA, A.H.C. Modelling Evapotranspiration by Remote Sensing Parameters and Agrometeorological Stations. In. Remote Sensing and Hydrology, Neale, CMU, Cosh, MH. Eds., IAHS Publ. 352, IAHS Press: Wallingford, UK, p. 154-157, 2012. Available from: https://www.alice.cnptia.embrapa.br/alice/bitstream/doc/946352/1/Heriberto.pdf

UNITED STATES GEOLOGICAL SURVEY - USGS. Landsat Project Description, 2020. Available from: http://landsat.usgs.gov/about_project_descriptions.php

VENANCIO, L.P., et al. Mapping within-field variability of soybean evapotranspiration and crop coefficient using the Earth Engine Evaporation Flux (EEFlux) application. *Plos one*. 2020, **15**(7), e0235620. https://doi.org/10.1371/journal.pone.0235620

VENANCIO, L.P., et al. Evapotranspiration mapping of commercial corn fields in Brazil using SAFER algorithm. *Science Agriculture*. 2021, **78**(4), e20190261. https://doi.org/10.1590/1678-992x-2019-0261

WAGLE, P. e GOWDA, P.H. Editorial for the Special Issue "Remote Sensing of Evapotranspiration (ET)". *Remote Sensing*. 2019, **11**(18), 2146. https://doi.org/10.3390/rs11182146

WARREEN, M.S., et al. Utilização do sensoriamento remoto termal na gestão de recursos hídricos. *Revista brasileira de Geografia Física*. 2014, **7**(1): 65-82. Available from: https://www.alice.cnptia.embrapa.br/alice/bitstream/doc/984718/1/3815.pdf

WILLMOTT, C.J., et al. Statistics for the evaluation and comparison of models. *Journal of Geophysics Research*. 1985, **90**, 8995-9005. https://doi.org/10.1029/JC090iC05p08995

WORLD PROCESSING TOMATO COUNCIL - WPTC. World production estimate of tomatoes for processing (in 1000 metric tonnes). Banco de dados, 2020. Available from: http://www.wptc.to/pdf/releases/WPTC%20World%20Production%20estimate%20as%20of%2027%20October%202016.pdf

XUE, J., et al. Evaluation of remote sensing-based evapotranspiration models against surface renewal in almonds, tomatoes and maize. *Agricultural Water Management*. 2020, **238**, 106228. https://doi.org/10.1016/j.agwat.2020.106228

ZHANG, X., et al. The Potential Use of Multi-Band SAR Data for Soil Moisture Retrieval over Bare Agricultural Areas: Hebei, China. *Remote Sensing*. 2016, **8**(1), 7. https://doi.org/10.3390/rs8010007

Received: 12 September 2023 | **Accepted:** 22 October 2024 | **Published:** 12 February 2025